

## DIRECT THRUST CONTROL SCHEME FOR A TUBULAR LINEAR BRUSHLESS PERMANENT-MAGNET ACTUATOR

Ioana-Cornelia VESE, Mircea M. RADULESCU

*Special Electric Machines and Light Electric Traction (SEMLET) Research Laboratory  
Faculty of Electrical Engineering, Technical University of Cluj-Napoca*

*P.O. Box 345, RO-400110 Cluj-Napoca 1, Romania  
E-mail: [ioana.vese@edr.utcluj.ro](mailto:ioana.vese@edr.utcluj.ro)*

**Abstract** – This paper investigates a suitable control scheme for tubular linear brushless permanent-magnet actuator (TLBLPMA) with the aim of revealing its efficiency in terms of fast and accurate dynamic response. Direct thrust control is proposed for a two-phase TLBLPMA prototype, with its peculiarities in terms of dynamic performance. Simulation results for the direct thrust-controlled TLBLPMA drive system are presented.

**Keywords:** *tubular linear permanent-magnet actuator, two-phase inverter topologies, direct thrust control*

### 1. INTRODUCTION

Direct Thrust Control (DTC) was implemented for the first time as a breakthrough in the control of linear electric drives, with particular emphasis on linear induction motors.

In this paper, the topology and switching pattern of the inverter supplying a two-phase tubular linear brushless permanent-magnet actuator (TLBLPMA) are firstly discussed. A proper DTC scheme for a TLBLPMA prototype is then proposed and simulated.

### 2. INVERTER-FED TWO-PHASE TLBPMA PROTOTYPE TOPOLOGY

The TLBLPMA prototype under study was provided by LinMot, Inc., a manufacturer of linear motors, guided actuators, and servo controllers [1].

The TLBLPMA prototype belongs to high-performance linear direct drives, and comprises two parts: the slider and the stator, having no connection between them, by brushes or cables. The linear motion is directly generated by the electromagnetic thrust, without the wear associated with mechanical gearboxes, belts, or levers. Extremely dynamic motion sequences can be obtained with a long lifespan. The TLBLPMA compact design is given by stator-integrated two-phase windings, Hall-effect position sensors and bearings [1].

The slider consists of a stainless steel tube, in which axially-magnetized NdFeB magnets are mounted, as shown in Fig. 1.



Figure 1: Two-phase TLBLPMA prototype under study (provided by LinMot, Inc.)

The main parameters of the two-phase TLBLPMA prototype, provided by the manufacturer are listed in Table 1.

Table 1: Main parameters of the TLBLPMA prototype under study

Symbol	Value	Parameter
$R$	20.6 $\Omega$	Phase resistance
$L_{d,q}$	2.7 mH	Phase inductance
$p$	9	Pole-pair number
$\tau_p$	0.0012 m	Pole pitch
$K$	22.1 N/A	Thrust constant
$\Psi_{PM}$	0.0085 Wb	PM-flux linkage

Since the two phase-windings are fixed within the stator, and orthogonally disposed, a two-axis stator-fixed orthogonal coordinate system can simply be adopted.

The TLBLPMA model is developed in direct-quadrature ( $d$ - $q$ ) axes reference frame, which rotates by the synchronous angular speed

$$\omega_{el} = \frac{\pi}{\tau_p} \cdot v \quad (1)$$

with respect to the stationary frame;  $v$  defines here the linear speed, and  $d$ -axis is aligned with the PM axis, whilst  $q$ -axis is aligned 90 degrees ahead in the direction of movement.

The voltage equations describing the two-phase TLBLPMA operation in the above-mentioned reference frame are

$$V_d = i_d R + \frac{d\psi_d}{dt} - v \cdot \frac{\pi}{\tau_p} \cdot \psi_q \quad (2)$$

$$V_q = i_q R + \frac{d\psi_q}{dt} + v \cdot \frac{\pi}{\tau_p} \cdot \psi_d$$

where  $V_d$  and  $V_q$  are the  $d$ -axis and  $q$ -axis components of the stator voltage space vector;  $i_d$  and  $i_q$  are the  $d$ -axis and  $q$ -axis components of the armature current vector;  $R$  is the armature-phase resistance. The armature winding  $d$ -axis and  $q$ -axis flux linkages  $\psi_d$  and  $\psi_q$  in (2) are expressed as

$$\begin{aligned} \psi_d &= i_d L + \psi_{PM} \\ \psi_q &= i_q L \end{aligned} \quad (3)$$

where  $L_d = L_q = L$  are the  $d$ - and  $q$ -axis armature inductances, and  $\psi_{PM}$  is the PM flux linkage.

The electromagnetic thrust developed in two-phase TLBLPMA yields from the energy balance equation, by identifying the electromagnetic power term; it can be shown that the motor produces an electromagnetic thrust that is position invariant [10].

$$F_{elm} = \frac{\pi}{\tau_p} (\psi_d \cdot i_q - \psi_q \cdot i_d) = \frac{\pi}{\tau_p} \cdot \psi_{PM} \cdot i_q \quad (4)$$

The mechanical equation of the model can be expressed in the differential form:

$$F_{elm} = M \cdot \frac{d^2 x}{dt^2} + B \cdot \frac{dx}{dt} + F_r \quad (5)$$

where  $M$  is the total moving mass, including load,  $B$  is the frictional constant and  $F_r$  includes the total effect of the residual thrusts due to cogging, stiction and eddy currents [2], [3].

Appropriate voltage-source inverter for high-performance drive system must be chosen for a two-phase TLBLPMA, and a review of the topologies is required for a good choice.

There are two main topologies of voltage-source inverter for proper feeding of two-phase motors [4], [5], i.e. the four-leg two-phase inverter (FLTPI), shown in Fig. 2, and the three-leg two-phase inverter (TLTPI) of Fig.3.

FLTPI topology comprises two single-phase full bridge inverters, i.e. eight switching modules. The two windings are separately connected to each of the two single-phase full-bridge inverters [5], [6]. It results in 16 switching states, 12 active and four zero states. The resulted space vectors are disposed, as depicted in the complex plane of Fig.4.

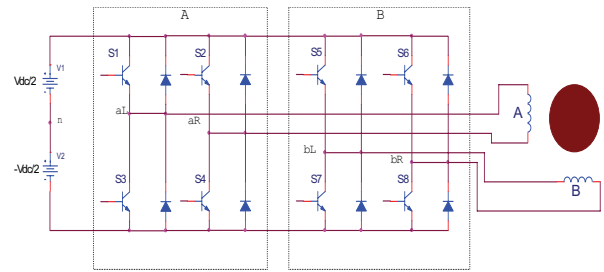


Figure 2: Four-leg two-phase inverter (FLTPI) topology

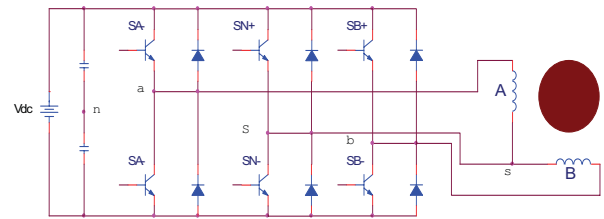


Figure 3: Three-leg two-phase inverter (TLTPI) topology

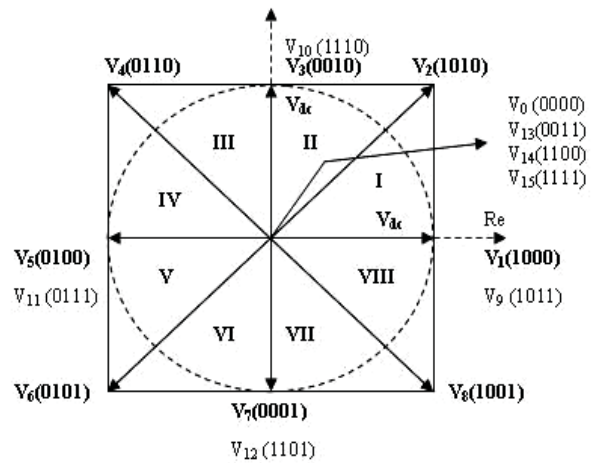


Figure 4: Space-vector distribution for FLTPI

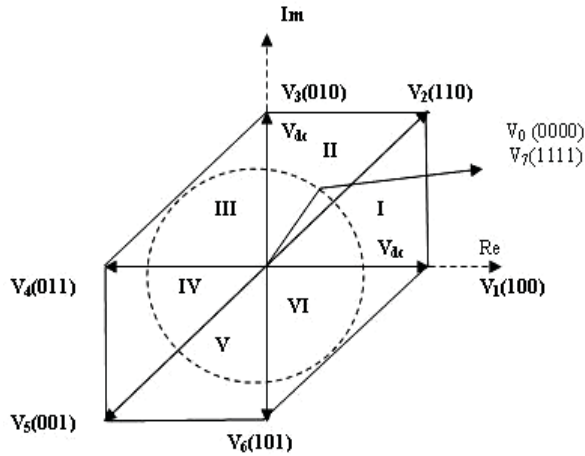


Figure 5: Space-vector distribution for TLTPM

In TLTPM topology, two inverter legs control the voltage of phase A and phase B, while the other leg controls the offset voltage  $V_{sn}$ . The eight switching states in this inverter form an asymmetrical hexagon, which has four space-vectors with  $V_{dc}$  length, and two space-vectors with  $\sqrt{2}V_{dc}$  length, and two zero space-vectors. In TLTPM, due to the absence of two diagonal space vectors, the circle inscribed in the polygon is  $\sqrt{2}$  times smaller in comparison with FLTPI, as shown in Fig. 5.

The circle inscribed inside each polygon of Figs. 4 and 5 denotes the locus of the reference voltage-vector amplitude.

The voltage space-vector may be expressed in a general form for the vectors aligned with the axis, the diagonal vectors and null vectors, respectively, for both inverter topologies as:

$$V_k = \begin{cases} V_{dc} \cdot e^{j(k-1)\frac{\pi}{4}} \\ \sqrt{2} \cdot V_{dc} \cdot e^{j(k-1)\frac{\pi}{4}} \\ 0 \end{cases} \quad (6)$$

The TLTPM provides output voltages that may have different amplitudes, which results in a slight difference on the phase quadrature. This creates drawbacks, especially in motors with low resistance and high self-inductance, at low speeds [2], [7].

From the comparison of both inverter topologies, it can be concluded that TLTPM is slightly superior in terms of maximum achievable output voltage. However, in the present study, the FPTPI topology was preferred for implementation.

### 3. DIRECT THRUST CONTROL (DTC) OF THE TWO-PHASE TLBLPMA

The basic concept of DTC used in linear electric motor drives is to control stator flux and thrust independently; it doesn't require any use of current loops, nor the coordinate transformation between stationary and synchronous frames, comparison with the conventional vector-controlled drives [2],[9]. Basically, the DTC-based linear drives require the knowledge of stator resistance only, thereby decreasing the associated sensitivity to parameter variations. In principle, classical DTC for a three-phase motor selects one of the six voltage vectors generated by a full-bridge voltage-source inverter in order to keep stator flux and torque within the limits of two hysteresis-band regulators.

Essentially, starting from the stator flux-linkage estimation

$$\psi(t) = \int (u - Ri) dt + \psi_0 \quad (7)$$

and neglecting the resistance voltage drop term, one can observe that the  $d$ -axis component of the voltage  $V_d$  is responsible for the increase/decrease of the flux amplitude.

From electromagnetic thrust equation (4), it can be noticed that an acceleration of the stator flux-linkage space-vector produces an increase of the thrust, provided that the PM-flux of the translator continues to move at the same speed.

Taking into account the active switching voltage vectors from Fig.4, the analysis of thrust and flux control in sector  $i$ , by virtue of the basic DTC, is presented in Fig.6.

The corresponding voltage vectors for each of the FLTPI eight sectors presented in Fig.4 can be expressed in an appropriate switching table (Table 2).

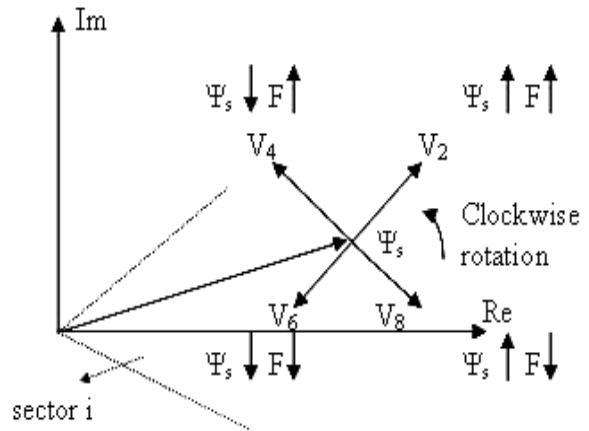


Figure 6: Flux and thrust control in the generic sector  $i$

Table 2: Switching table for FLTPI topology

STATUS		SECTOR							
$\varepsilon_\psi$	$\varepsilon_F$	I	II	III	IV	V	VI	VII	VIII
1	1	V <sub>2</sub>	V <sub>3</sub>	V <sub>4</sub>	V <sub>5</sub>	V <sub>6</sub>	V <sub>7</sub>	V <sub>7</sub>	V <sub>8</sub>
1	-1	V <sub>8</sub>	V <sub>1</sub>	V <sub>2</sub>	V <sub>3</sub>	V <sub>4</sub>	V <sub>5</sub>	V <sub>6</sub>	V <sub>7</sub>
X	0	0	0	0	0	0	0	0	0
-1	1	V <sub>4</sub>	V <sub>5</sub>	V <sub>6</sub>	V <sub>7</sub>	V <sub>8</sub>	V <sub>1</sub>	V <sub>2</sub>	V <sub>3</sub>
-1	-1	V <sub>6</sub>	V <sub>7</sub>	V <sub>8</sub>	V <sub>1</sub>	V <sub>2</sub>	V <sub>3</sub>	V <sub>4</sub>	V <sub>5</sub>

The input values of a two-phase TLBLPMA DTC scheme are the reference thrust and the reference flux linkage. The errors yielded from the comparison with their actual values represent the inputs for two hysteresis comparators, which provide two digital outputs that can be either zero or one, as further explained.

A current-based model is proposed and implemented in this section. Actually, for the studied TLBLPMA prototype, the analytical estimations of the thrust and stator flux yielding the current-based estimation model are represented by

$$F_a = \frac{\pi}{\tau_p} \left\{ \psi_{PM} \left[ i_b \cos\left(\frac{\pi}{\tau_p} x\right) - i_a \sin\left(\frac{\pi}{\tau_p} x\right) \right] \right\}$$

$$\psi_a = L_a \cdot i_a + \psi_{PM} \cdot \cos\left(\frac{\pi}{\tau_p} x\right)$$

$$\psi_b = L_b \cdot i_b + \psi_{PM} \cdot \sin\left(\frac{\pi}{\tau_p} x\right)$$

(8)

$$\psi_s = \sqrt{(\psi_a)^2 + (\psi_b)^2}$$

where  $\frac{\pi}{\tau_p} x$  stands for the angle between  $d$ -axis and

$a$ -phase axis, and represents, in fact, a specific control parameter in the control scheme implemented for the two-phase TLBLPMA.

#### 4. SIMULATION RESULTS

The dynamic behaviour of the DTC two-phase TLBLPMA drive system was studied using a mathematical implementation in Matlab-Simulink software. The implemented model was created using the real parameters given by the prototype's manufacturer.

The DTC two-phase TLBLPMA scheme was implemented using the previously described algorithm, as well as the FLTPI topology and switching pattern.

The position information subsequently used in the calculation of the sector, in which the flux vector lays, represents an important issue. For the two-phase TLBLPMA, it yields from the integration of the linear speed. Furthermore, taking into account the linear movement periodicity for TLBLPMA, an analytical calculation is generated in this block.

The actual values of the electromagnetic thrust and stator linkage flux are compared with their references, the results entering two hysteresis comparators.

Signals from torque and flux linkage hysteresis controllers, as well as the position information are indexing elements for the FLTPI switching table, the essential element of the DTC.

The position response and linear velocity are displayed in Fig.7, with emphasis of TLBLPMA motion reversal.

Flux linkage trajectory is plotted in Fig.8, whereas thrust response is given in Fig.9.

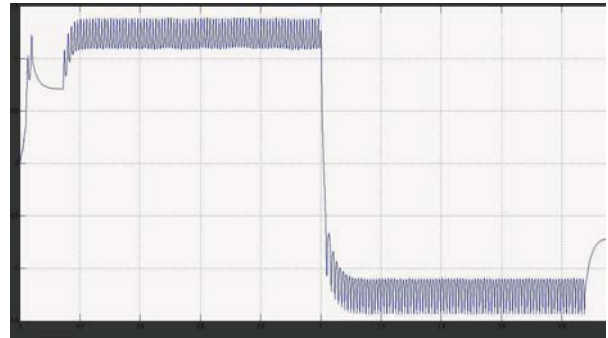


Figure 7: DTC two-phase TLBLPMA simulated position and speed response

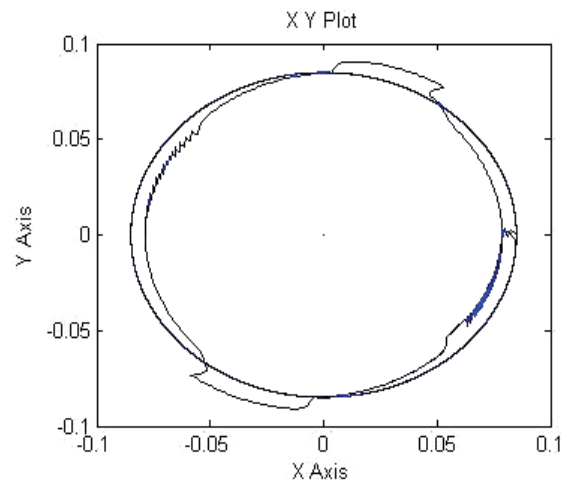


Figure 8: DTC two-phase TLBLPMA stator flux-linkage locus

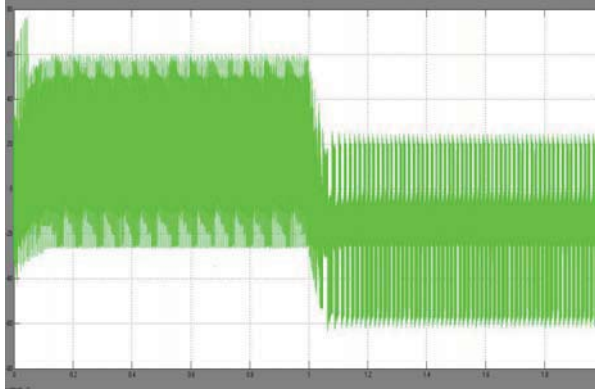


Figure 9: DTC two-phase TLBLPMA thrust simulated response

There is a noticeable ripple due to the lack of modulation in the voltage outputs of the inverter feeding the two-phase TLBLPMA.

A SVM approach [8], [9] is thus envisaged for TLBLPMA drive applications in order to reduce the undesired ripple in the electromagnetic thrust and phase currents by generating modulated voltages from the feeding inverter.

## 5. CONCLUSIONS

DTC scheme for a two-phase TLBLPMA prototype was implemented. Feeding inverter topology and appropriate switching pattern were described, along with the mathematical modelling of the two-phase TLBLPMA.

A current-based model was implemented in order to estimate TLBLPMA quantities, and to avoid the inaccuracies introduced in a conventional voltage-based model.

Finally, dynamic simulation results have revealed the DTC scheme suitability for direct-drive, constant-force, industrial applications of the two-phase TLBLPMA prototype.

## REFERENCES

- [1] [www.Linmot.com](http://www.Linmot.com)
- [2] V. Kremer, Z.Q. Zhu, D. Howe, "Indirect and direct force control of a two-phase tubular permanent magnet machine", *IEEE Trans. Power Electron.*, vol.22, no.2, pp.654-662, March 2007.
- [3] I.B. Salem, L. El Amraoui Ouni, M. Benrejeb, F. Gillon, P. Brochet, "Modelling and control strategies for a tubular permanent-magnet linear synchronous motor drive system", *Electromotion EPE Chapter 'Electric Drives' Joint Symposium*, 1-3 July 2009, Lille, France.
- [4] D.H. Jang, "PWM methods for two-phase inverters", *IEEE Ind. Applicat. Mag.*, pp.50-61, Mar/Apr, 2007.
- [5] C.B. Jacobina, M.B. Correa, A.M.N. Lima, E.R.C. da Silva, "AC motor drive system with a reduced-switch-count converter", *IEEE Trans. Ind. Applicat.*, vol. 39, no. 5, pp. 1333-1341, 2003.
- [6] M. B. R. Correa, C. B. Jacobina, A. M. N. Lima, and E. R. C. da Silva, "A three-leg voltage source inverter for two-phase ac motor drive systems," *IEEE Trans. Power Electron.*, vol. 17, pp. 517-523, July 2002.
- [7] M. Correa, C. Jacobina, and A. Lima, "Rotor-flux-oriented control of a single-phase induction motor drive," *IEEE Trans. Ind. Electron.*, vol. 47, no. 4, pp. 832-841, Aug. 2000.
- [8] D. Casadei, G. Serra, "Implementation of a direct torque control algorithm for induction motors based on discrete space vector modulation", *IEEE Trans. Power Electron.*, Vol. 15, pp.769-776, 2000.
- [9] V. Kremer, Z.Q. Zhu, D. Howe, "Analysis and application of two-phase space-vector modulation to a novel tubular PM motor", *Proc. 4th Int. Symp. Linear Drives Ind. Applicat. - LDIA 2003*, 8-10 Sept. 2003, Birmingham, UK.
- [10] B. Gysen, K.J. Meessen, J. Paulides, E.A. Lomonova, "Semi-Analytical Calculation of the Armature Reaction in Slotted Tubular Permanent Magnet Actuators", *IEEE Transactions on Magnetics*, Vol. 44, Issue 11, Part 1, Nov. 2008, pp. 3213 - 3216.